

Contents

1	Introduction	1
2	Experiment	5
2.1	Construction of stable light path	5
2.1.1	CRL parameter determination	5
2.1.2	Reduce beam jitter	7
2.2	Construction of the combined system	8
2.3	Determination of spot parameters	9
2.4	Collection of micro-focus X-ray scattering data	11
3	Application	12
3.1	Microstructure of ringed spherulites	12
3.2	The skin and core structure of the fiber	14
4	Conclusion	14

1 Introduction

Macromolecules are characterized by their long-chain structure, including molecular chain unit and conformation on the angstrom scale, lamella on the nanometer scale and spherulites on the micron scale. Nowadays, synchrotron radiation small angle X-ray scattering (SAXS) and wide angle X-ray diffraction (WAXD), as a non-destructive, highly statistically averaged structure analysis method, have been extensively used in crystalline polymer research area. For instance, information on grains in crystalline polymer, micro-domains in blended polymers and the shape, size and distribution of cavities and cracks can be obtained by guinier scattering. Information on orientation, thickness and crystalline fraction of crystalline layer and the thickness of the amorphous layer can be obtained by long-period measurement.

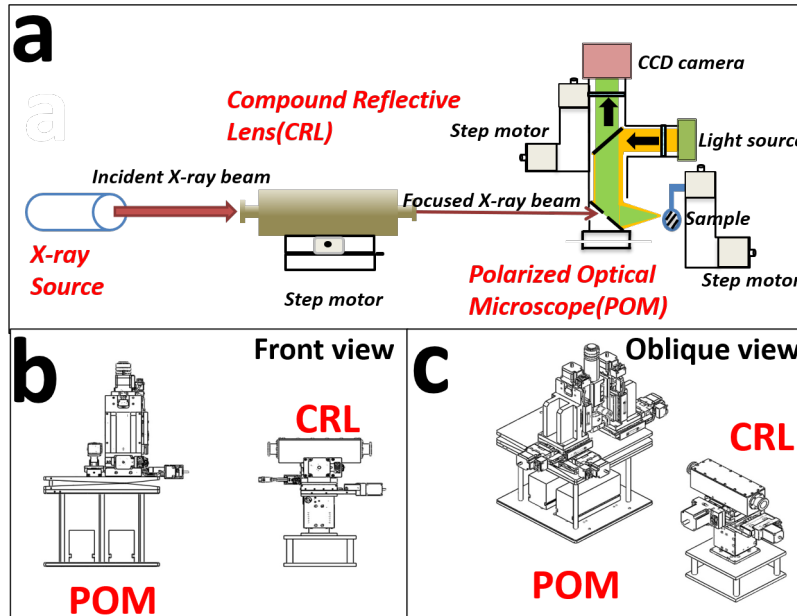


Fig. 1. Whole system.

10 To further study the internal structure of polymers, two test conditions are essential. Firstly, considering
 11 the size of specific structural unit, the size of the X-ray spot can not be too large. For instance, in spherulites
 12 research, an X-ray spot with a size of $5\mu\text{m} \times 5\mu\text{m}$ is required. A small spot provides sufficient spatial
 13 resolution when the structure of macromolecules are characterized by the SAXS method. Secondly, to
 14 match the characterization result with the real structure, it is a critical measure to confirm the real-time
 15 exact position of the X-ray incident beam on polymer crystal.

16 As described, the X-ray spot needs to be focused and located.

17 To improve the spatial resolution of the synchrotron radiation experiment, nearly all the world's ad-
 18 vanced synchrotron radiation facilities focus the X-ray spot in the micron or even sub-micron level. Rep-
 19 resentative beam line stations include PETRA III P03, SSRF BL15U1. However, limited by the distance
 20 between the sample and the detector, SAXS experiments can not be implemented on these stations. Conse-
 21 quently, it is necessary to build an independent optical system with the functions of X-ray micro-focusing

22 and precise spot positioning on the existing SAXS beam line.

23 The main component used for X-ray beam focusing includes a Kirkpatrick-Baez mirror, Fresnel zone
24 plates, Capillary optical lens and Compound refractive lenses. In synchrotron radiation area, Kirkpatrick-
25 Baez mirror(K-B mirror) and Compound refractive lenses(CRL) are more widely used. In practice, ad-
26 vantages of K-B mirror are aberration-free imaging on both horizontal and vertical planes, no dispersion,
27 high energy, high reflectivity and low flux losses. However, there are some non negligible disadvantages.
28 Micro-beam focusing by K-B mirror needs to be achieved by adjusting the interval mirrors and multi-axis
29 spatial attitude, including: the angle of incident X-ray on the mirrors, the vertical angle of the two mirrors,
30 spatial parallelism of two vertical cylinders. The deployment of K-B mirror changes the original optical
31 path. Thus, the K-B mirror, as an off-axis device, increases the complexity of the installation of all the
32 experimental equipment. This is unfavorable for the entire micro-focusing experiment process.

33 Compound refractive lenses(CRL) are comprised of a series of single lenses arranged in a linear array to
34 achieve X-ray focusing in the energy range of 5-40 keV. As shown in [Fig. 2](#), the most widely used CRL are
35 parabolic CRL. The parabolic CRL has a parabolic surface that rotates around the axis of symmetry to form
36 a parabola. It can focus X-rays in two dimensions without causing aberrations in theory. Compared to K-B
37 mirror, CRL does not alter the original optical path propagation direction. CRL has excellent high temper-
38 ature stability, simple and compact structure and low requirements for lens' surface roughness. Moreover,
39 CRL is not difficult to adjust and relatively insensitive to vibration. The most obvious disadvantage of CRL
40 is its low transmission efficiency. Owing to the small aperture of the diaphragm and the high absorbed rate
41 of X-ray for CRL, the intensity of focused light will drop by one to two orders of magnitude than original
42 light. Despite this, the luminous flux can be maintained at $10^{10} \sim 10^{11}$ phs/s after CRL micro-focusing. It
43 can be proved in [subsubsection 2.1.1](#). This flux is enough for the structure research of crystalline polymers.

44

45 Polarized optical microscopy(POM) is commonly used in polymer crystal morphology research. POM
46 is a simple method to distinguish the change of growth direction of crystals in the film plane and to check

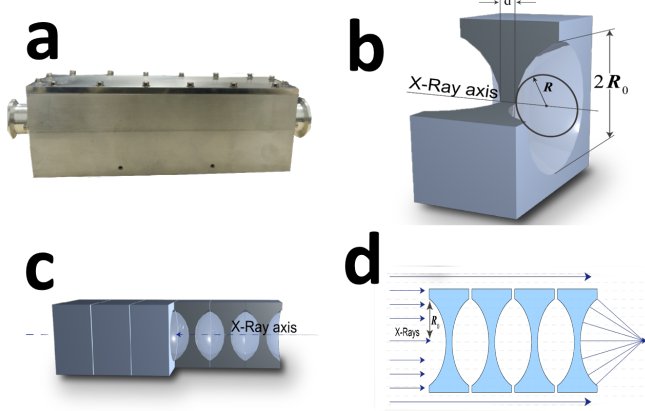


Fig. 2. Structure of Compound reflective lenses

47 whether there exists twisting of crystals[1]. Fig. 3 is a schematic diagram of the disassembly of a POM.
 48 When the polarized light generated by the polarizer and the analyzer enters the anisotropic polymer crystal,
 49 birefringence occurs, and the crystal contrast is provided by the coherence of the polarized light. Different
 50 crystal forms of polymers, such as spherulites, string crystals, stretched chain crystals, transverse crystals,
 51 etc., all have anisotropic optical properties, so their crystal morphology, size, number, etc. can be observed
 52 clearly with a POM.

53 In this passage, a combined system of micro-focusing SAXS and POM is proposed. A series of pa-
 54 rameters of the device is adjusted, and the device is used to characterize the crystalline morphology and
 55 microstructure of related polymers.

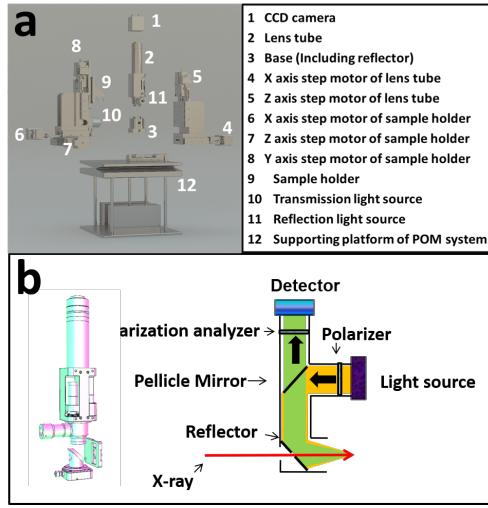


Fig. 3. POM overall disassembly and lens cone disassembly.

Table 1. Parameters of several common single lens

Radius $R/\mu\text{m}$	Aperture $2R_0/\mu\text{m}$	Area $\pi R_0^2/\text{mm}^{-2}$
200	881	0.609
100	623	0.305
50	440	0.152

56 2 Experiment

57 2.1 Construction of stable light path

58 2.1.1 CRL parameter determination

59 In order to obtain the designed X-ray microbeam, CRL's parameters are necessary to be determined first.
 60 The parameter mainly include material, geometric size and number of pieces. Commonly used CRL is
 61 aluminum and beryllium. Basing on the theory of atomic physics, materials with low atomic number have
 62 less absorption of X-rays. In this system, a beryllium CRL is chosen because the X-ray energy has to be
 63 preserved as much as possible.

64 There are three common single lenses. The main geometric parameters of them are listed in [Table 1](#).

65 First, CRL with a radius of $50 \mu\text{m}$ is selected to calculate the relevant parameters.

66 Transmittance refers to the ratio of the light intensity after passing through the lens and the light intensity
 67 without passing through the lens. It can be calculated by Eq. 1[2]:

$$T_p = \frac{\int_0^{2\pi} d\theta \int_0^{R_o} e^{-\mu ND(r)} r dr}{\int_0^{2\pi} d\theta \int_0^{R_o} r dr} = \frac{1 - e^{-a}}{a} e^{-\mu Nd} \quad (1)$$

68 In Eq. 1, $a = \mu NR_o^2/R$, R and R_o are given in Table 1, N is the number of lens, d is the minimum thickness
 69 of a single mirror. For parabolic lenses, d can be calculated by Eq. 2:

$$D(r) = d + 2 \times \frac{r^2}{2R} \quad (2)$$

70 The maximum thickness $D(r)$ of the selected CRL is 2 mm. Substituting $D(r)$ and $r = R_o$ into the Eq. 2, d
 71 equals 1.032 mm.

72 Considering the actual situation of shed size and pipeline layout, the designed image distance is about
 73 400 mm and so is the focal length. The focal length under the approximate condition of thin lens can be
 74 calculated by Eq. 3 :

$$f = R/2N\delta \quad (3)$$

75 N is the amount of lenses, δ is real part of refractive index to 1 offset. δ can be calculated by Eq. 4 [3]:

$$\delta = \frac{2\pi\rho r_o}{k^2} \quad (4)$$

76 ρ is electron number density, r_o is the electronic classical radius and k is wave vector. For beryllium in
 77 12KeV, δ is 2.36393×10^{-6} . When N is set to 30, the focal length is 352.5 mm. This value meets the
 78 requirements described above. Substituting $N = 30$ and $d = 1.032$ into the Eq. 1, T_p equals 0.327.

79 The flux of photons after passing through the lenses can be calculated by the following equation:

$$I = i \times T_p \times R \quad (5)$$

80 i is the flux of incident X-ray. In BL19U2, under a current intensity of 220 mA, $i = 2.5 \times 10^{12}$ photons/s,
81 R is defined as the photon acceptance rate and equals 0.0598 in BL19U2. Substituting these values into the
82 Eq. 5, I equals 4.89×10^{10} photons/s. This value is enough to study the structure of crystalline polymers.

83 For lens with a radius of $100\mu\text{m}$ and $200\mu\text{m}$, after the same calculation, N is 60 and 120. Although
84 a lens with a larger radius of curvature can be used to obtain a slightly larger flux, the number of lenses
85 required is greatly increased. Comprehensive consideration, using 30 lenses with a radius of $50\mu\text{m}$ is the
86 best choice.

87 2.1.2 Reduce beam jitter

88 Due to the thermal load caused by the high-power beam to the monochromator crystal and the vibration of
89 the monochromator crystal caused by the liquid nitrogen cooling system of the monochromator, the current
90 spot of the BL19U2 is differed by about 10%, which will affect the strength stability of X-ray micro beam.

91 A processing software is compiled which integrates light intensity position data collection, data process-
92 ing (calculation of beam center), data smoothing and filtering, PID control algorithm and control interface.

93 Advanced FPGA technology is applicable to design and implement a fuzzy adaptive PID controller. Beam
94 position which is collected by the PID control loop in real time is compared with the set value. Then the
95 comparison error is sent to the PID controller to calculate the control value through the PID control algo-
96 rithm. Subsequently, the comparison error is input to the actuator of the monochromator piezo to adjust
97 the piezo angle of the second crystal in real time. This operation realizes the constant feedback system of
98 the beam center position and the constant light intensity feedback system. Finally, it is realized that the
99 closed-loop control of the beam position and suppress low the beam drift of the frequency band to realize

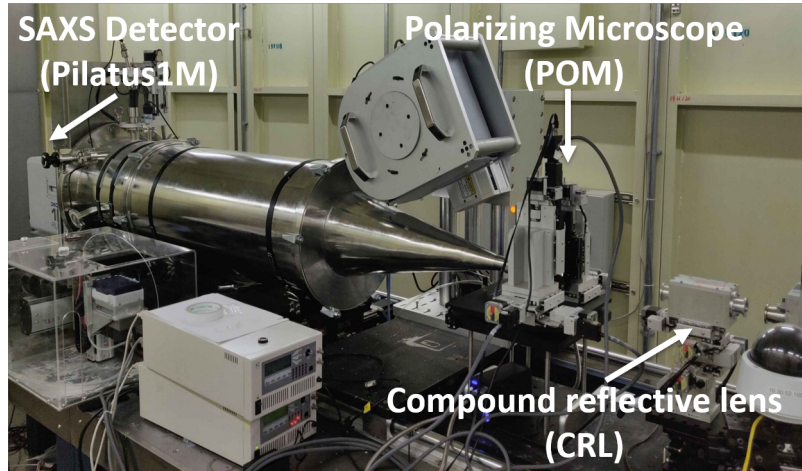


Fig. 4. Site map of the combined system.

100 the stabilization of the BL19U2. Thus, the impact of beam jitter on the intensity of the focused beam is
 101 lowered.

102 2.2 Construction of the combined system

103 Fig. 1 is the schematic diagram of the structure of synchrotron radiation X-ray micro-focusing polarized
 104 microscopy system. The combined system has one micro-focusing component and an in situ polarized light
 105 microscope system. After the incident X-ray is focused by the CRL, it will pass through the light hole on
 106 the lower side of the POM and the sample, then the scattered signal will be received by the detector. The
 107 on-site construction diagram of the system is shown in Fig. 4.

108 As shown in Fig. 1, the CRL is mounted on a motorized platform. Including three-dimensional transla-
 109 tional electric platform (x , y , z three directions), one-dimensional swing stage (P angle) and one-dimensional
 110 rotating platform (R angle). The posture of CRL can be adjusted in five spatial dimensions.

111 The structure of POM used in the system is shown in Fig. 3. As shown in Fig. 3b, the optical system of
 112 POM mainly consists of the following parts: a polarizer and analyzer that use ordinary white light sources
 113 to generate polarized light; a half mirror located in the middle of the lens barrel; A flat mirror located at the

¹¹⁴ bottom of the lens barrel. The detector at the top is utilized to collect images. In this system, the detector
¹¹⁵ selects a Charge-coupled device(CCD) camera.

¹¹⁶ As shown in Fig. 3a, the in situ POM system is also installed on a motorized support platform. A
¹¹⁷ stepping motor (4~5) installed on the side of the lens body realizes the translational adjustment of the lens
¹¹⁸ barrel in two dimensions. Similarly, the stepping motor (6~8) on the side of the sample holder realizes
¹¹⁹ its translational adjustment in three dimensions. The supporting platform (12) can be further divided into
¹²⁰ three layers: the uppermost layer is a one-dimensional swing stage and a rotating table, the middle layer is
¹²¹ a two-dimensional (horizontal) translational electric platform, and the lowest layer is a three-dimensional
¹²² translational electric platform. Through the adjustment devices in all the above dimensions, the five spatial
¹²³ dimensions of the entire optical system can be adjusted.

¹²⁴ 2.3 Determination of spot parameters

¹²⁵ Once the combined system is installed in beam line, the beam can be adjusted. The main purpose of beam
¹²⁶ adjustment is threefold: first, to ensure the connectivity of the integrated optical path, to ensure that X-rays
¹²⁷ can pass through the system correctly. A series of elements on the fixed light path of the beam line is used to
¹²⁸ adjust the primary light spot, and then the light path is adjusted using the POM and CRL spatial dimensions.
¹²⁹ The current value of the ionization chamber can determine whether there is sufficient X-ray flux to irradiate
¹³⁰ the sample. The second purpose is to verify whether the CRL is accepted to focus the primary spot to a
¹³¹ sufficiently small spot size. Only when the size is basically in line with the theoretical value to achieve a
¹³² sufficiently small spatial resolution, can the microstructure of the research system be characterized; the third
¹³³ is to adjust the position of the light spot to the center of the field of view, while adjusting the angle of the
¹³⁴ plane mirror to make the polarized light that reaches the sample after being reflected twice by the half mirror
¹³⁵ and the plane mirror is focused on the X-ray at this point in the sample. The detection point of the sample
¹³⁶ is placed in the center of the field of view, and the detection position will not shift even if the magnification
¹³⁷ of the polarizing microscope is changed. To achieve the latter two purposes, we need to observe the spot in

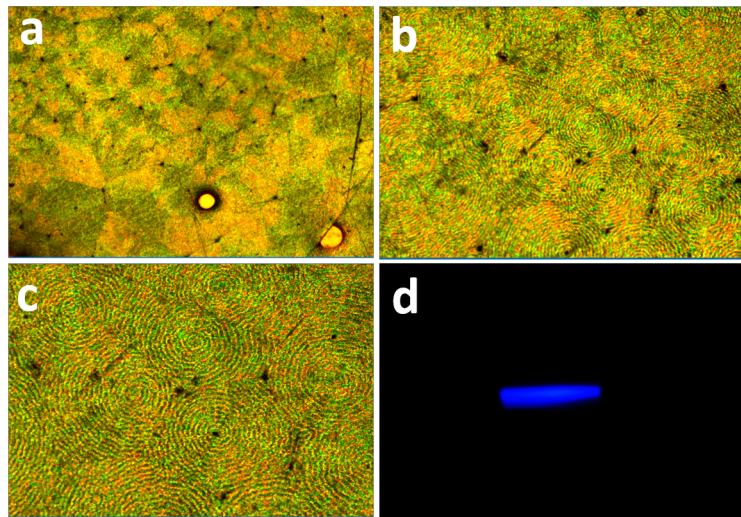


Fig. 5. Result of commissioning POM on site

138 real time under POM. For this reason, we install a cesium iodide crystal on the sample stage. Cesium iodide
 139 crystal has the characteristic of emitting fluorescence under X-rays, so it is also called scintillation crystal.
 140 In this system, the X-ray spot position is calibrated by the fluorescence spectrum generated by cesium iodide
 141 under POM.

142 Step motors used in this system are all produced by Kohzu Corporation. Positioning accuracy can reach
 143 1um, which is enough for precise spatial position adjustment. Adjust the CRL posture so that the incident
 144 X-ray can pass through the lenses correctly and be focused. Then adjust the y-direction motor of the POM
 145 sample stage, so that the scintillation crystal is correctly focused and imaged in the field of view of the
 146 polarizing microscope. Finally, set the x and z direction motors to move the center of the field of view to
 147 the fluorescent spot. In the PC imaging software, a cross ruler will be displayed to provide assistance in
 148 positioning.

149 The theoretical size of the focus spot is about $5\mu\text{m} \times 5\mu\text{m}$. In check to see whether the error between the
 150 actual size and the theoretical calculation is within the allowable range, two methods are used. As shown

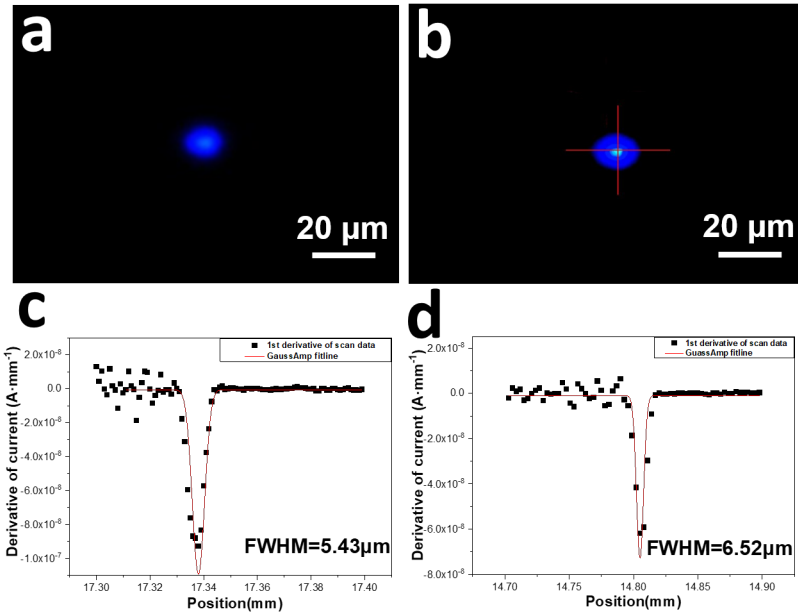


Fig. 6. Result of CRL micro-focus (facula and flux)

in Fig. 6a and Fig. 6b, the first is to visually observe through imaging software and use a ruler to make rough measurements. This method is fairly intuitive and fast, but the accuracy is insufficient. The second method is Gaussian fitting by using current data of ionization chamber. Basing on related theories, the flux of X-rays determines the intensity of the current in the ionization chamber. FWHM of the $\frac{dI}{dx} \sim x$ curve(first derivative of the ionization chamber current to displacement) represents the spot size. Representative fitting results of this system are shown in Fig. 6c and Fig. 6d. The FWHM of the fitted peak is calculated to be $5.43\mu\text{m} \times 6.52\mu\text{m}$. This value basically achieves the expected effect.

2.4 Collection of micro-focus X-ray scattering data

After adjusting the size and position of the light spot, it can be utilized to characterize the micro-domain structure of related polymer crystals. First, determine the position that needs to be characterized under the POM, and then use the motor installed on the platform to remove the visible light source. Passing in

₁₆₂ synchrotron X-rays to collect scattered signals. At the SSRF-BL19U2 line station, X-rays with an energy of
₁₆₃ 12keV are often utilized, and the distance between the sample and the detector is 2700mm. The scattering
₁₆₄ signal is collected by Pilatus1M detector (981×1043 pixel, with a pixel size of $172\mu\text{m} \times 172\mu\text{m}$).

₁₆₅ **3 Application**

₁₆₆ In order to verify the feasibility of the entire combined system, the spherulites with annulus and fibers with
₁₆₇ a sheath-core structure are used as research examples. Micro-focused X-ray spot is used for micro-area
₁₆₈ resolution, and the scattering information of small structures that cannot be obtained by ordinary small-
₁₆₉ angle scattering experiments can be obtained.

₁₇₀ **3.1 Microstructure of ringed spherulites**

₁₇₁ Spherulites are the most common morphological structure of polymer materials, and they play a vital role
₁₇₂ in the physical, chemical and mechanical properties of polymer materials. Its multi-level structure is com-
₁₇₃ plicated, and many basic scientific issues related to its structure have yet to be further explored. At present,
₁₇₄ in the study of the microstructure of zonal spherulites, there are several scientific problems that need to be
₁₇₅ explained urgently. The first problem is the correlation between the growth axis of the polymer ring-belt
₁₇₆ spherulites and the torsion chirality of the lamellae. One theory is that the growth axis affects the chirality
₁₇₇ of the lamella torsion by changing the pressure distribution on the lamella plane. Micro-focus X-ray can be
₁₇₈ used to determine the growth axis of each region and the tilt torsion behavior of the mapping crystal plane
₁₇₉ along the growth axis, revealing the correlation between the crystal growth axis and the lamella torsion chi-
₁₈₀ rality. It can provide a scientific basis for clarifying the transfer behavior of chirality between the multi-level
₁₈₁ structure of polymer spherulites. The second problem is the cross nucleation of polymer spherulites during
₁₈₂ the crystallization. Through micro-focus X-ray, the crystalline transformation information at the front of
₁₈₃ spherulite growth are monitored in situ, including crystal plane, orientation, whether there is a transition

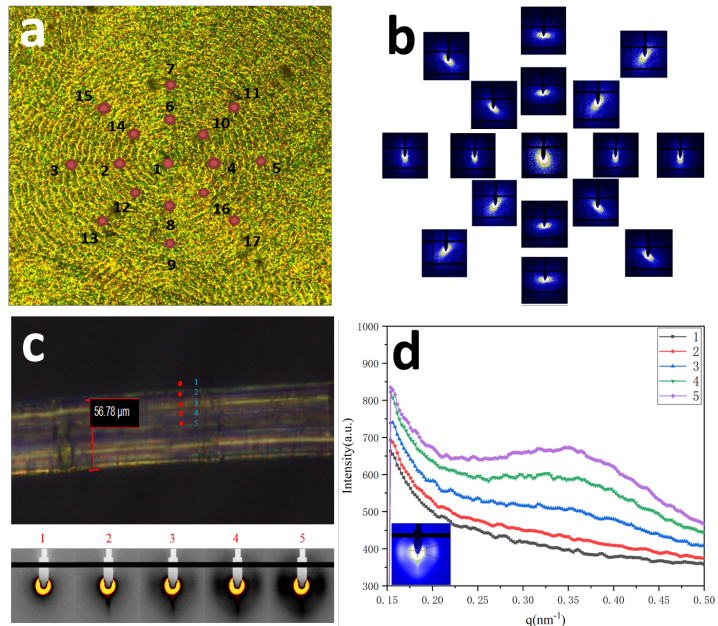


Fig. 7. The application sample of the system

184 (gradient) zone to reveal the cross nucleation mechanism in polymer crystals, and clarify multiple crystal
 185 types the correlation and the similarities and differences between polymer cross nucleation and traditional
 186 cross nucleation of small molecule.

187 Ringed-spherulites were chosen to verify the usability of the micro-focusing polarizing microscope sys-
 188 tem. Micro beam X-ray scans were especially informative. As shown in Fig. 7a, the initial growth site (1)
 189 of the ringed-spherulites was first calibrated, and the micro-focus SAXS characterization was performed on
 190 this point. Subsequently, 8 sites were uniformly selected and characterized on a certain circumference of the
 191 ring-belt spherulites. In order to eliminate contingency, a total of 16 sites (2-17) in two different circles were
 192 selected, and SAXS characterization was also performed. The two-dimensional image of the SAXS result is
 193 shown in Fig. 7b, and it can be seen from Fig. 7b that the distribution of the scattering intensity at different
 194 sites is different. The scattering intensity at the center of the spherulites is equal in all directions. However,
 195 in all directions around the ringed-spherulites, there is a certain orientation, which also reflects the periodic
 196 changes in the arrangement of the lamellae on the ringed-spherulites. Through the precise characterization

¹⁹⁷ of the ringed-spherulites by micro-focused X-rays, experimental results with certain differences have been
¹⁹⁸ obtained. The above examples can support the usability of the system.

¹⁹⁹ **3.2 The skin and core structure of the fiber**

²⁰⁰ For fiber materials, the skin layer and the core layer of the fiber will have certain structural differences due
²⁰¹ to the temperature and shear flow field factors in the preparation process. Some fibers have small diameters,
²⁰² and conventional SAXS methods cannot accurately characterize the structure of the skin or core layer. The
²⁰³ interval of taking points is about $5\mu\text{m}$. Micro-focused X-rays can accurately distinguish the skin layer from
²⁰⁴ the core layer and even the transition layer, and use the scattering data to study the structural differences.

²⁰⁵ As shown in Fig. 7c, the micro-beam X-rays irradiate the detection points of the skin and core of the
²⁰⁶ fiber. The corresponding scattering data is shown in Fig. 7d.

²⁰⁷ **4 Conclusion**

²⁰⁸ In this paper, based on the development trend of multi-scale structure characterization methods of poly-
²⁰⁹ mer materials, for the first time, a set of CRL-POM combined device was built on a synchrotron radiation
²¹⁰ line station to realize the scattering characterization based on optical micro-area resolution. The research
²¹¹ methods and technical routes used in this experiment have been tested many times. The feasibility of the
²¹² experimental system has also been verified by a variety of material research systems. The system can pro-
²¹³ vide theoretical guidance for the molecular structure and high-performance design of related materials in
²¹⁴ the industry. At the same time, it also provides a new characterization platform for the SSRF Small angle
²¹⁵ X-ray scattering station, and a new combination structure characterization method for internal and external
²¹⁶ teams conducting polymer crystal structure research.

217 **References**

- 218 [1] Jun Xu, S. Z., Haimu Ye & Guo, B. Organization of twisting lamellar crystals in birefringent banded
219 polymer spherulites: A mini-review. *Crystals* **7** (2017).
- 220 [2] Lengeler, B. *et al.* Imaging by parabolic refractive lenses in the hard X-ray range. *Journal of Synchrotron
221 Radiation* **6**, 1153–1167 (1999). URL <https://doi.org/10.1107/S0909049599009747>.
- 222 [3] Als-Nielsen, J. & McMorrow, D. *Elements of Modern X-ray Physics* (Wiley, 2011). URL <https://books.google.co.jp/books?id=rlqlbowlTRMC>.
- 223